JOURNAL OF VIROLOGY, Apr. 1992, p. 2369–2377
0022-538X/92/042369-09$02.00/0

Vol. 66, No. 4

# Role of the Apical Stem in Maintaining the Structure and Function of Adenovirus Virus-Associated RNA

KENNETH H. MELLITS,† TSAFRIRA PE'ERY, AND MICHAEL B. MATHEWS*
*Cold Spring Harbor Laboratory, P.O. Box 100, Cold Spring Harbor, New York 11724*

Received 3 October 1991/Accepted 15 December 1991

**Adenovirus virus-associated (VA) $RNA_I$ maintains efficient protein synthesis during the late phase of infection by preventing the activation of the double-stranded-RNA-dependent protein kinase, DAI. A secondary structure model for VA $RNA_I$ predicts the existence of two stems joined by a complex stem-loop structure, the central domain. The structural consequences of mutations and compensating mutations introduced into the apical stem lend support to this model. In transient expression assays for VA RNA function, foreign sequences inserted into the apical stem were fully tolerated provided that the stem remained intact. Mutants in which the base of the apical stem was disrupted retained partial activity, but truncation of the apical stem abolished the ability of the RNA to block DAI activation in vitro, suggesting that the length and position of the stem are both important for VA RNA function. These results imply that VA $RNA_I$ activity depends on secondary structure at the top of the apical stem as well as in the central domain and are consistent with a two-step mechanism involving DAI interactions with both the apical stem and the central domain.**

Adenovirus virus-associated (VA) $RNA_I$ is required for the maintenance of protein synthesis at late times during infection. This small RNA antagonizes the cell's antiviral defense mechanism by inhibiting the activation of the interferon-induced, double-stranded-RNA (dsRNA)-dependent protein kinase, DAI. In the absence of VA $RNA_I$, activated DAI phosphorylates eukaryotic initiation factor 2 (eIF-2), impeding the initiation of protein synthesis (reviewed in reference 16).

Examination of the secondary structure of VA $RNA_I$ in solution by using the nuclease sensitivity technique suggests that it contains two stems, the apical stem and the terminal stem, separated by a complex stem-loop structure termed the central domain (18). The VA RNA species of different adenovirus serotypes display similar but not identical structures (13). Mutagenic and other analyses indicate that the central domain is required for the inhibition of DAI activation by dsRNA and implicate the apical stem in the binding of VA RNA to DAI (5, 6, 17, 18).

To define the features of the apical stem that are important for the function of VA RNA, we have investigated the structural and functional consequences of mutations within the apical stem. The data indicate that when foreign sequences are inserted into this region, full activity is retained provided that the foreign sequences preserve base pairing in the apical stem and do not severely disturb the central domain. Substitutions that preserve some pairing in the apical stem, and do not disrupt the central domain, display partial activity. Thus, the preservation of secondary structure in the apical stem appears to be more important than primary sequence per se for VA $RNA_I$ function. Results obtained with deletion mutations support this conclusion and suggest that the apical stem structure must be distanced from the central domain for the molecule to block DAI activation in vitro. These findings are consistent with the hypothesis that VA $RNA_I$ is a specialized effector containing two functionally distinct domains which combine to allow efficient protein synthesis during adenovirus infection.

* Corresponding author.
† Present address: Gene Expression Laboratory, Imperial Cancer Research Fund, Lincoln's Inn Fields, London WC2A 3PX, United Kingdom.

## MATERIALS AND METHODS

**Construction of mutants.** All mutants constructed here were generated by oligonucleotide-directed mutagenesis (12, 28), using *Escherichia coli* CJ 236. Mutants *ls*1a to -e were generated within the VA $RNA_I$ gene of plasmid pMHVA (18), and deletion mutants *del*49-60, *del*53-80, and *del*73-84 were generated within the VA $RNA_I$ gene of plasmid pT7VA (19). The *dl*1, *ls*1, *ls*3, *ls*5 (18), and A2dl2 (4) mutations were also introduced into the VA $RNA_I$ gene of plasmid pT7VA. The efficiency of site-specific mutation was approximately 50%. Oligonucleotides were synthesized by using a 380-A DNA synthesizer (Applied Biosystems), and mutants were analyzed by dideoxy sequencing (24) using a kit (United States Biochemical Corporation).

**Determination of RNA secondary structure.** The secondary structures of wild-type and mutant VA RNAs were determined by the RNase sensitivity technique (18). Each mutant RNA was labeled at its 5′ or 3′ end and subjected to partial digestion under conditions such that most RNA molecules were not digested and the remainder were cleaved only once. We employed the single-stranded specific RNase $T_1$, *Bacillus cereus* RNase, RNase $U_2$, and RNase $T_2$ (specific for G residues, pyrimidines, A residues, and any exposed base, respectively), as well as nuclease $V_1$ from cobra venom (specific for helical and stacked nucleotides). Digestion products were analyzed in denaturing gels run for various lengths of time to resolve all regions of the RNA molecules, and the positions and intensities of nuclease cleavages were noted. RNA secondary structure models were derived by manual folding and the use of a computer program which incorporated both empirical data and estimates of energies inherent in base pairing (9, 29).

**Transient expression assay.** The mutants were tested for function by transfecting monolayers of 293 cells in duplicate with wild-type (pMHVA) or mutant plasmids (18). The cells were infected 24 h later with Ad5*dl*331, a mutant virus that is unable to synthesize VA $RNA_I$. The ability of each plasmid

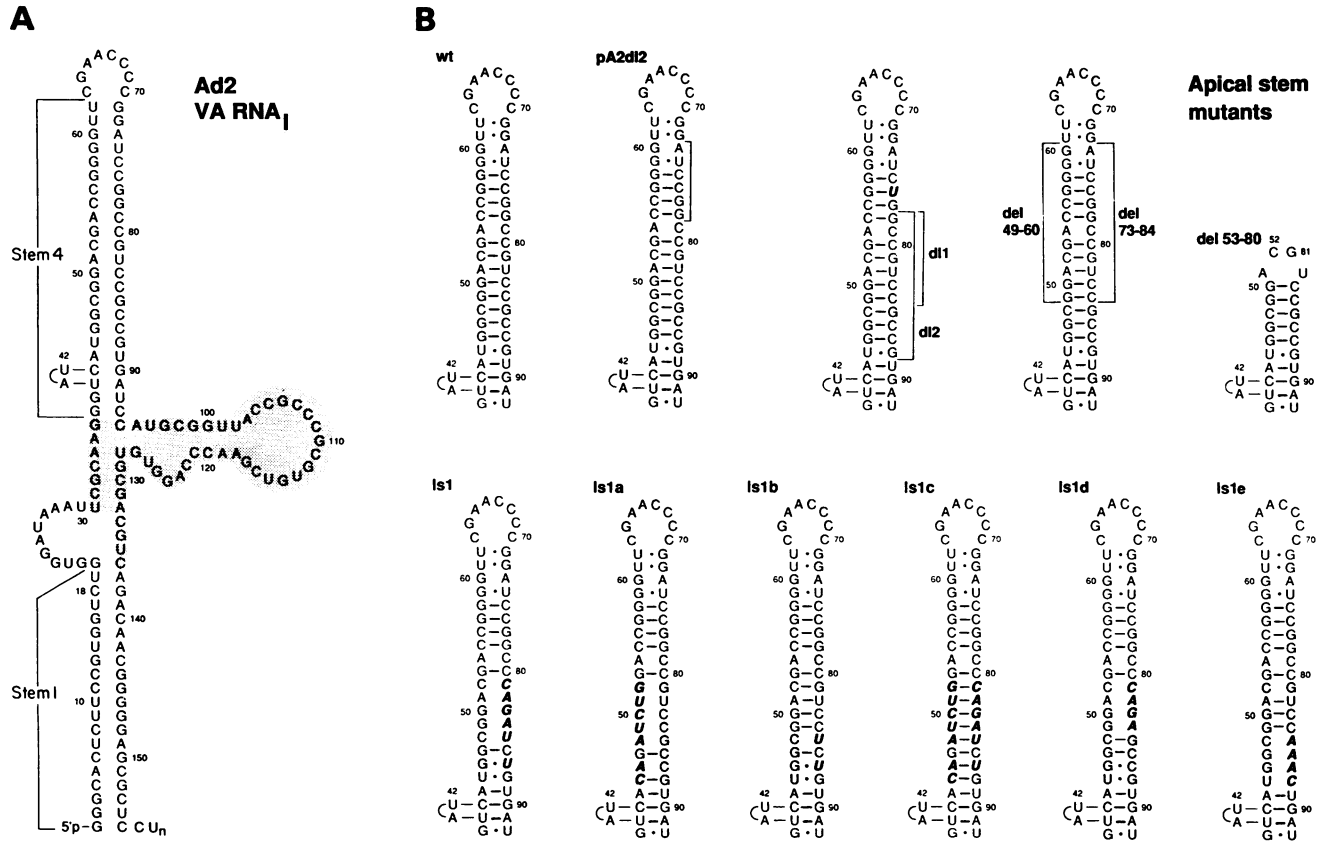


FIG. 1. Structure of VA RNA$_I$ and sequences of mutants. (A) Model for Ad2 VA RNA$_I$ (redrawn from references 17 and 18) showing the central domain (stippled), apical stem (stem 4), and terminal stem (stem 1). (B) Sequences of mutant RNAs superimposed on the stem 4 structure of wild-type Ad2 VA RNA$_I$, assuming no structural rearrangements consequent upon mutation. Base substitutions are in boldface; deletions are bracketed.

to rescue protein synthesis in *trans* was quantified after pulse-labeling the cells with [$^{35}$S]methionine at 48 h post-transfection. At the same time, the accumulation of each mutant RNA was determined by Northern (RNA) blot analysis.

**Kinase assay.** Wild-type and mutant VA RNAs were purified by sequential fractionation through denaturing and nondenaturing 8% polyacrylamide–7 M urea gels, followed by cellulose CF-11 chromatography (19). The VA RNA was then incubated with DAI (purified to the hydroxylapatite stage [11]) either in the presence or absence of reovirus dsRNA (courtesy of A. J. Shatkin) as described previously (19). The bands containing autophosphorylated DAI were excised and subjected to scintillation counting or were quantified by using the AMBIS Beta-Scanning System (Automated Microbiology Systems, Inc.).

## RESULTS

Principally on the basis of nuclease sensitivity analysis, we developed a model for the secondary structure of wild-type adenovirus type 2 (Ad2) VA RNA$_I$ (18) which is largely consistent with the perturbations resulting from the introduction of deletions and substitutions in the molecule (5, 6, 17, 18). The structure contains two imperfectly duplexed stems, the terminal and apical stems (stem 1 and stem 4), each of 20 to 25 bases, joined by a complex stem-loop structure, the central domain (Fig. 1A). The central domain is required for inhibition of DAI activation (5, 17, 18), while the apical stem (stem 4) is responsible for the efficient binding of VA RNA to DAI (17). Base pairing in the apical stem differs sharply from that predicted by secondary structure programs alone (1, 27). For example, the predicted structure contains a run of six G-C base pairs between nucleotides (nt) 55 to 60 and 67 to 72; these are calculated to confer greater stability than the experimentally determined pairing scheme, which nevertheless lacks this six G-C run. To test the structural model and explore the role of apical stem sequences, we constructed three sets of mutants in this region by site-directed mutagenesis.

**Substitution mutants.** Deletions within the apical stem encompassing nt 73 to 78 and 78 to 84 (mutations A2dl2 and *dl*1) are compatible with full activity in transient expression assays, suggesting that the region between nt 73 and 84 is nonessential for VA RNA function (18). Nuclease sensitivity analysis indicated that the structures of the A2dl2 and *dl*1 RNAs are perturbed only in the apical stems near the sites of mutation. In A2dl2, the stem accommodates the deletion by rearranging in such a way as to form six G-C pairs at its apex, as in the computer-predicted structure, while in *dl*1 the apical loop expands considerably in size (17). Neither deletion significantly affects the structure of the central domain. Extension of the *dl*1 deletion by 4 nt to nt 88 (in mutant *dl*2) ablates function (18) (Fig. 1B), as does a linker-scanning

mutation (*ls*1) that substitutes the same bases, nt 81 to 88, with a *Bgl*II linker. In these cases, structural analysis revealed widespread disturbances involving both the area of mutation (stem 4) and the central domain (17, 18).

The region between nt 85 and 88 is altered in both defective mutants (*dl*2 and *ls*1) but not in either of the functional mutants (*dl*1 and pA2dl2), suggesting that it constitutes a critical region in the middle of stem 4. These nucleotides might compose a sequence that is essential in itself, or they might be critical for the stability of essential secondary structure in stem 4 or elsewhere in the molecule, particularly in the central domain. To examine these possibilities, we initially constructed a series of three mutations, *ls*1a to -c, in the vector pMHVA, which permits expression in human cells by RNA polymerase III (Fig. 1B). First, to determine the effect of primary sequence alterations within this region, we made a mutant that contains the subset of *ls*1 substitutions lying between nt 85 and 88. The resulting mutant, *ls*1b, contains only two changes, a G→U transversion at nt 85 and a C→U transition at nt 87. The latter would be expected to allow pairing to the G residue at nt 46, and these relatively slight changes were not expected to perturb the secondary structure to a significant degree. Second, to test the hypothesis that it is the secondary structure formed by nt 85 to 88 rather than their sequence per se that is required for VA $RNA_I$ function, we made mutant *ls*1c by introducing a *Bgl*II linker between nt 45 and 52 of *ls*1. This mutant was expected to restore wild-type structure through compensating base mutations in stem 4. Third, as a control, the linker sequence was introduced into the wild-type molecule between nt 45 and 52. The resulting mutant, *ls*1a, was expected to contain a 6-nt mismatch in stem 4 and to display a perturbed secondary structure.

Nuclease sensitivity analysis largely bore out these expectations. Two mutants, *ls*1b and *ls*1c, gave cleavage patterns almost identical to that of wild-type VA $RNA_I$, indicating that the secondary structures of these RNAs closely resemble that of the wild-type RNA (Fig. 2A and B). The *ls*1a cleavage pattern was significantly different, particularly in that nt 46 to 53 and 79 to 86 were substantially more susceptible to attack by single-strand specific nucleases. This is diagrammed in Fig. 2C, in which the cleavages are superimposed on the wild-type structure, and in Fig. 2D, which gives a secondary structure model for *ls*1a RNA. Unlike the case with its counterpart, *ls*1 (Fig. 2E and F), the disruption of *ls*1a structure resulting from mismatches in stem 4 was largely confined to the area of the mutations, which displayed extensive melting and formed a bifurcation. Partial melting was also observed at the base of the apical stem (nt 37 to 39), but the central domain remained intact.

To assess the functional consequences of these mutations, we investigated the capacity of the mutant RNAs, introduced by plasmid transfection, to rescue protein synthesis in cells infected with the mutant adenovirus Ad5*dl*331. This virus is unable to synthesize VA $RNA_I$, and consequently protein synthesis fails during the late phase (25). The ability of *ls*1b to rescue protein synthesis was unimpaired (Fig. 3 and Table 1), showing that the *ls*1b sequence changes are not independently detrimental in themselves, although they are extremely deleterious to the structure and function of the molecule when combined with substitutions within the neighboring "nonessential" sequences (nt 81 to 84) in mutant *ls*1 (Fig. 3 and Table 1). We conclude that the defect in *ls*1 is not due solely to the changes at nt 85 and 87.

Mutant *ls*1c, containing the compensating base changes, increased protein synthesis 3.2-fold compared with levels in cells transfected with a control plasmid (Table 1). Presumably because it contains mutations near the internal control region required for VA RNA transcription (4, 7, 23, 26), *ls*1c RNA accumulated to only 30% of wild-type levels (Fig. 3B, Table 1). When the input of wild-type DNA was reduced so that comparable levels of wild-type VA $RNA_I$ and *ls*1c RNA were produced, *ls*1c rescued protein synthesis as well as wild-type VA $RNA_I$ (data not shown), indicating that the compensating mutations restore both the structure and function of the molecule.

In the rescue assay, *ls*1a stimulated translation 2.1-fold, significantly less well than wild-type VA $RNA_I$ (Table 1). The mutant RNA accumulated to lower levels than wild-type VA RNA, probably because this mutation also affects the B box of the internal control region (though it is unclear why *ls*1a accumulated to higher levels than *ls*1c). When this differential accumulation was taken into account by varying the amount of plasmids in the transfection assay, *ls*1a RNA was found to rescue protein synthesis 40 to 50% as efficiently as wild-type VA $RNA_I$. We conclude that the structural integrity of the midsection of stem 4 contributes to, but is not absolutely required for, the maintenance of VA RNA function.

In contrast to *ls*1a RNA, which retains considerable functional and structural integrity, the corresponding mutant *ls*1 is severely defective (18) (Fig. 3 and Table 1). The defect cannot be attributed simply to primary sequence changes, since the same mutations are present (albeit in duplex form) in *ls*1c RNA, which retains function. Structural analysis shows that *ls*1 RNA has suffered a radical rearrangement (Fig. 2E and F), possibly because the CAGA sequence of the *Bgl*II linker has invaded stem 2, pairing with nt 17 to 20 and creating widespread disturbances in stem 4 (which has opened out) and the central domain (which has reorganized). A second possibility is that some sequence or structure at the base of stem 4 contributes to the stability of the central domain and hence to VA RNA function.

**Further substitution mutants.** To distinguish between these alternatives, we generated two additional substitution mutants (Fig. 1B). Mutant *ls*1d contains the nucleotides CAGA substituted for nt 81 to 84; this sequence was expected to remain unpaired, as in *ls*1, and so could potentially disturb structure elsewhere in the molecule. In mutant *ls*1e, the sequence AAAC replaces the wild-type sequence UCUG from nt 85 to 88. This change was designed to create the maximal perturbation in the pairing system at the base of stem 4.

Analysis of the secondary structures of these two mutants is illustrated in Fig. 4A. As expected, the *ls*1d substitution resulted in a bulge at the site of mutation. Furthermore, the mutation caused perturbations at the apex of the molecule, consistent with the formation of a hairpin loop containing six G-C base pairs as in A2dl2 RNA (17). There was also a rearrangement at the base of stem 4, forming a bifurcation (Fig. 4B and C), and some minor cleavage changes in the central domain. Nevertheless, the overall cleavage pattern was more compatible with the wild-type structure than with the grossly perturbed *ls*1 structure (Fig. 2F), indicating that an unpaired CAGA sequence is not invariably deleterious. Similarly, minor rearrangements of VA $RNA_I$ structure resulted from the AAAC substitution in *ls*1e. The structure of stem 4 was altered at the site of mutation, forming a large bifurcation (Fig. 4D and E). Again, the apex of stem 4 rearranged to form a hairpin loop similar to that of A2dl2 RNA. The secondary structure of the central domain was largely unaffected by the *ls*1e mutation, although new nucle-

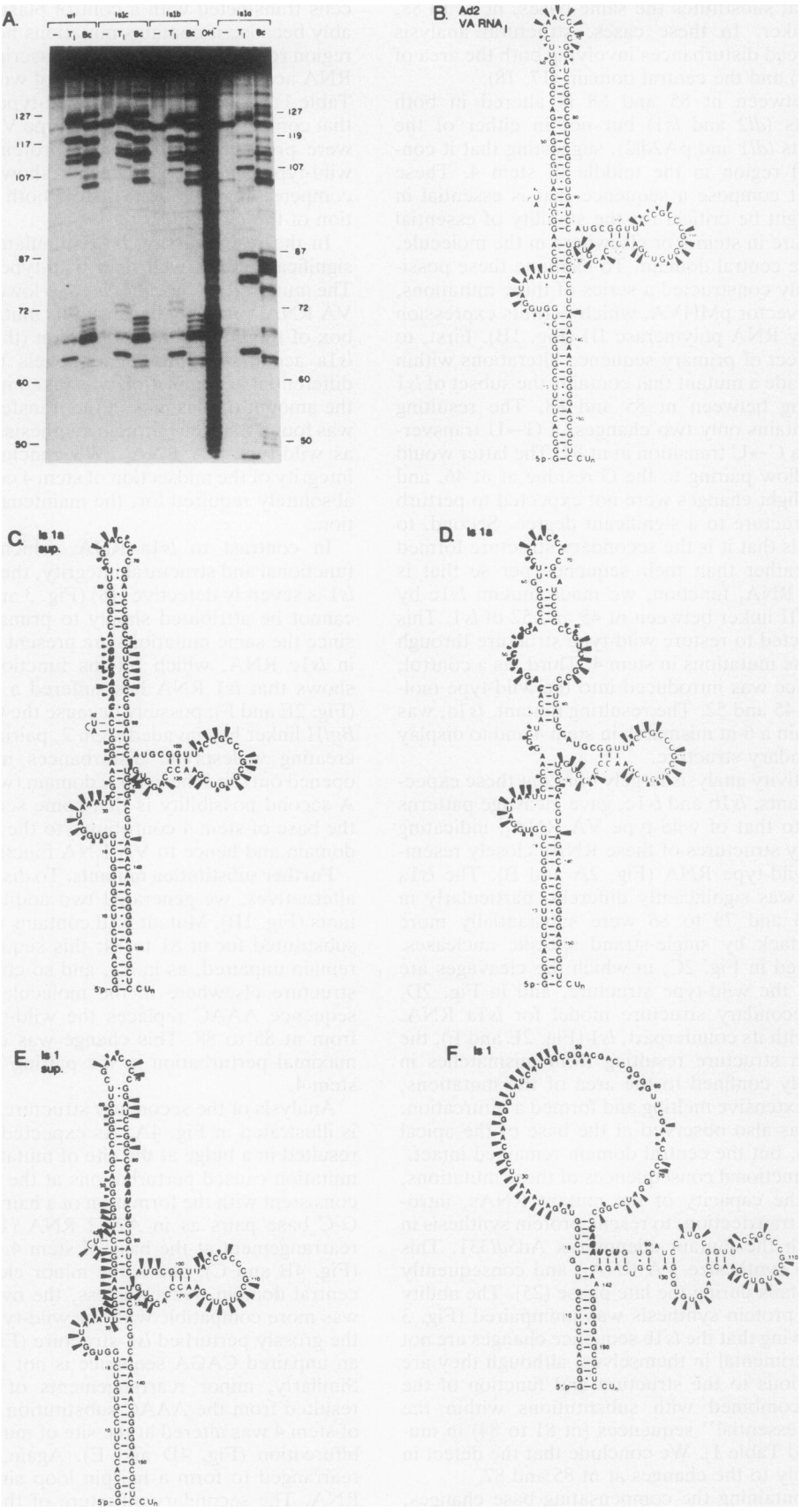
A.
wt
Is1c
Is1b
Is1a
– T1 Bc – T1 Bc – T1 Bc OH⁻ – T1 Bc
127
117
107
87
72
60
50
127
119
107
87
72
60
50
B. Ad2 VA RNA I
C. Is 1a sup.
D. Is 1a
E. Is 1 sup.
F. Is 1

FIG. 2. Secondary structure of mutant *ls*1a to -c VA RNAs. (A) Nuclease sensitivity analysis of Ad2 VA $RNA_I$ (wt) and three mutants. Each 5'-end-labeled RNA was partially digested with RNase $T_1$ or *B. cereus* RNase (Bc) or was left undigested (−), and it was then fractionated in an 8% polyacrylamide–7 M urea gel. Nucleotide positions are marked, and a ladder of randomly digested VA $RNA_I$ is shown ($OH^-$). (B through F) Models deduced from cleavage data by manual and computer-assisted folding. Sites sensitive to the single-stranded specific RNase $T_1$, *B. cereus* RNase, RNase $U_2$, and RNase $T_2$ are indicated; large arrowheads, small arrowheads, and dots indicate strong, weak, and very weak cleavages, respectively. Panel B displays the nuclease-sensitive sites for wild-type Ad2 VA $RNA_I$. Nuclease sensitivities of the mutants and of *ls*1a and *ls*1 are shown superimposed on the Ad2 wild-type structure (panels C and E, respectively) or redrawn on the basis of nuclease cleavage (panels D and F, respectively). Boldface italic letters represent changes from wild-type sequence. (Panels B, E, and F are redrawn from reference 17; note that the cleavage site at nt 135 has been moved to nt 136.)

ase $V_1$ cleavages appeared between nt 32 and 35, as in *ls*1d RNA.

In the functional assay, *ls*1d and *ls*1e rescued protein synthesis in Ad5*dl*331-infected cells, but not as effectively as wild-type VA $RNA_I$ (Fig. 5 and Table 1). For reasons that are unknown, both *ls*1d and *ls*1e RNAs accumulated to higher levels than wild-type VA $RNA_I$ (Table 1 and Fig. 5A). In separate titration experiments, translational stimulation reached a plateau between 10 and 15 μg of wild-type pMHVA per plate, indicating that further increase in the steady-state RNA levels probably makes no additional contribution to the translational stimulation seen (data not shown). We conclude that perturbations at the base of stem 4 reduce but do not eliminate the ability of VA RNA mutants to rescue protein synthesis.

**Deletion mutants.** Although VA $RNA_I$ appears to require duplex structure to inhibit the activation of DAI, this requirement allows for some flexibility. To define the minimal requirements for stem structure and to approach the smallest functional VA $RNA_I$ molecule, we generated a mutant that was designed to permit the formation of a short apical stem comprising only 7 bp (*del*53-80; Fig. 1B). This mutation removes the B box required for transcription by RNA polymerase III, so it was introduced into the vector pT7VA, which allows efficient production of VA RNA by using T7 RNA polymerase (19). At the same time, we produced two other deletion mutants which remove roughly equivalent portions from either side of stem 4. Mutant *del*73-84 lacks the presumptively nonessential region corresponding to the combined A2dl2 and *dl*1 deletions, while *del*49-60 lacks the sequences which pair to nt 73 to 84 in wild-type VA RNA (Fig. 1B). The structures of these mutant VA RNAs were probed as above, and their function was assessed by measuring their ability to inhibit the activation of DAI in vitro.

Nuclease sensitivity analysis showed that the secondary structure of *del*53-80 RNA is roughly the same as that of wild-type VA RNA. As expected, the deletion caused truncation of the apical stem, leaving a short hairpin loop containing a stem of approximately 11 bp, including a small bifurcation at its base (Fig. 6A). Only minor perturbations occurred within the central domain, including new nuclease $V_1$ cleavages at nt 33 to 35.

Consistent with the perturbations brought about by the substitution mutations discussed above, *del*73-84 and especially *del*49-60 exhibited more drastic structural changes. The deletion of nt 73 to 84 still permitted the formation of a stable hairpin between nt 43 and 90, albeit with a shift to the six G-C pairing scheme as in A2dl2 and a bulge between nt 49 and 54 (Fig. 6C). Changes at the base of stem 4 resulted in a

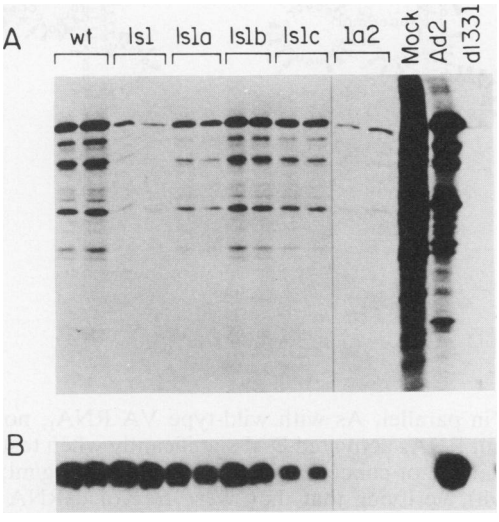


FIG. 3. Rescue of protein synthesis by mutants *ls*1a to -c. (A) Monolayers of 293 cells were transfected with 15 μg of the plasmids indicated, infected with Ad5*dl*331, and pulse-labeled with [$^{35}$S]methionine (18). Equal portions of each labeled cell extract were analyzed by sodium dodecyl sulfate-polyacrylamide gel electrophoresis and fluorography. Control plates were uninfected (Mock) or infected with Ad2 or Ad5*dl*331. All plasmid constructs are based on pMHVA (wt), which contains the gene for Ad2 VA $RNA_I$. Plasmid p1a2 served as a negative control; it contains a *Bgl*II linker between nt 56 and 84, disrupting the transcriptional B box. (B) Equal portions of cytoplasmic RNA from each culture were fractionated in a formaldehyde-agarose gel and transferred to nitrocellulose membrane. The blot was probed with nick-translated pMHVA DNA. An autoradiogram of the VA RNA region is shown.

TABLE 1. Efficiency of rescue and expression[a]

| Plasmid | Protein synthesis[b] | VA RNA accumulation[c] |
|---|---|---|
| Control | 1.0 | 0.0 |
| Set 1 | | |
| pMHVA | 6.3 ± 1.2 | 1.0 |
| pMHls1 | 1.2 ± 0.5 | 1.1 ± 0.1 |
| pMHls1a | 2.1 ± 0.4 | 0.64 ± 0.04 |
| pMHls1b | 7.7 ± 2.0 | 1.0 ± 0.2 |
| pMHls1c | 3.2 ± 0.2 | 0.3 ± 0.05 |
| Set 2 | | |
| pMHVA | 5.1 ± 0.9 | 1.0 |
| pMHls1d | 3.2 ± 0.6 | 1.5 ± 0.5 |
| pMHls1e | 3.5 ± 0.3 | 2.1 ± 0.5 |

[a] Values are averages of several transfection experiments, with standard deviations indicated.

[b] Ratio of the hot trichloroacetic acid-precipitable radioactivity incorporated by cells transfected with the plasmid specified to that incorporated by cells transfected with a plasmid which does not synthesize VA $RNA_I$ (pAT153 or p1a2).

[c] Ratio of radioactivity in the band corresponding to VA RNA in Northern blots from cells transfected with the specified plasmid to that from cells transfected with pMHVA.

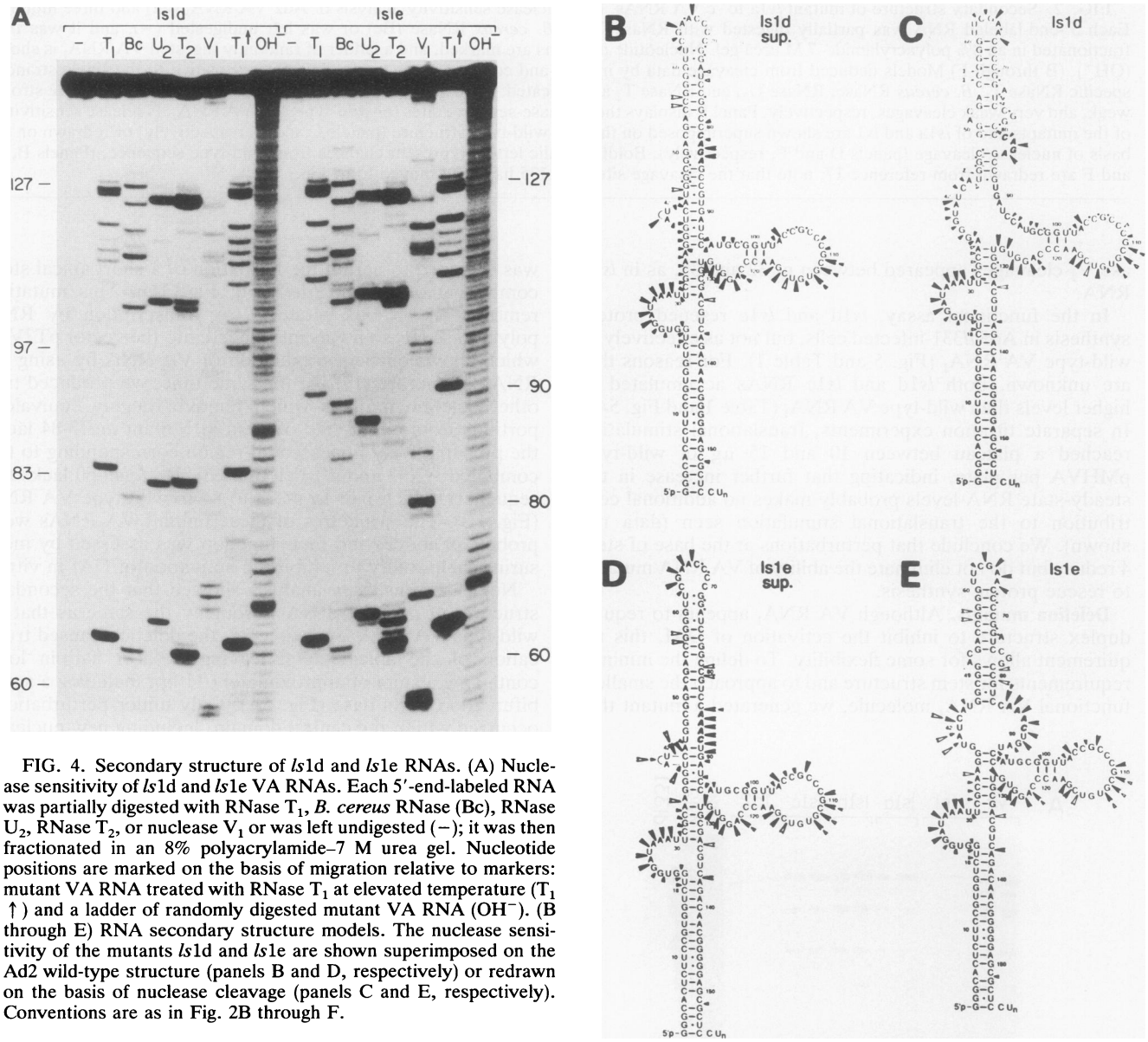


FIG. 4. Secondary structure of *ls*1d and *ls*1e RNAs. (A) Nuclease sensitivity of *ls*1d and *ls*1e VA RNAs. Each 5′-end-labeled RNA was partially digested with RNase $T_1$, *B. cereus* RNase (Bc), RNase $U_2$, RNase $T_2$, or nuclease $V_1$ or was left undigested (–); it was then fractionated in an 8% polyacrylamide–7 M urea gel. Nucleotide positions are marked on the basis of migration relative to markers: mutant VA RNA treated with RNase $T_1$ at elevated temperature ($T_1$ ↑) and a ladder of randomly digested mutant VA RNA ($OH^-$). (B through E) RNA secondary structure models. The nuclease sensitivity of the mutants *ls*1d and *ls*1e are shown superimposed on the Ad2 wild-type structure (panels B and D, respectively) or redrawn on the basis of nuclease cleavage (panels C and E, respectively). Conventions are as in Fig. 2B through F.

bifurcation around nt 37 to 40 and 91 to 94, but the central domain appeared extant despite some alterations in single- and double-strand specific cleavage sites. Interestingly, this mutant displayed both nuclease $V_1$ and single-strand specific cleavages at nt 110 to 112 and 116. This distinctive pattern is characteristic of wild-type VA $RNA_I$ and mutants that are functional in vivo (17, 18). The presence of overlapping single- and double-strand specific cleavage sites is not uncommon in highly structured RNAs, and it may reflect a particularly stable tertiary structure within the central domain (10). By contrast, deletion of nt 49 to 60 induced gross rearrangements of the apical stem and central domain (Fig. 6B). In these regions, *del*49-60 RNA exhibited few resemblances to the wild-type structure, although the other end of the molecule appeared to be unaltered.

The mutant RNAs were tested for their abilities to inhibit the dsRNA-dependent autophosphorylation of DAI; for comparison, several mutants previously tested in transient expression and in vitro binding assays (17, 18) were examined in parallel. As with wild-type VA $RNA_I$, none of the mutant RNAs activated DAI significantly when tested over a wide range of concentrations (5 ng/ml to 50 μg/ml; data not shown), verifying that they were free of dsRNA contaminants (19). Representative results from kinase inhibition assay experiments are illustrated in Fig. 7, and a number of these were quantified.

To various degrees, all the RNAs inhibited DAI activation in vitro, especially at the highest concentrations tested (20 and 50 μg/ml), but in most cases there were clear differences between the functional and nonfunctional RNAs. Ad2 VA $RNA_I$ and A2dl2 RNA function in transient expression assays and bind to DAI efficiently (17, 18). These RNAs inhibited DAI activation in vitro almost completely at 50 and 20 μg/ml and were significantly inhibitory at 5 μg/ml (Fig. 7). Of the deletion mutants, only *del*73-84 RNA approached this degree of efficiency: it blocked the activation of DAI nearly

completely at high concentration but was slightly impaired at lower concentrations, 5 and 1 μg/ml (Fig. 7). This result confirms that function is compatible with slight disturbances in the apical stem, although there is a small loss in efficiency of inhibition.

The mutant *ls*1 RNA does not function in transient expression assays and does not bind efficiently to DAI (17, 18). Correspondingly, this RNA did not block DAI activation efficiently, although it gave approximately 65% inhibition at the highest RNA concentration (50 μg/ml). The RNAs of deletions *del*49-60 and *del*53-80 behaved similarly, indicating that neither the gross deformation of the apical stem and central domain in *del*49-60 nor the severe shortening of the apical stem in *del*53-80 is consistent with VA RNA function. Since in the latter molecule the stem is no shorter than in some other mutants that retain at least partial function (e.g., *ls*1a, -d, and -e), we conclude that there is an additional requirement for the stem to be distanced from the central domain.

The mutant *dl*1, which is anomalous in that it functions in transient expression assays but does not bind efficiently to DAI (17, 18), is also relatively ineffective at blocking DAI activation in vitro (Fig. 7). This apparent anomaly can perhaps be resolved if the in vitro assays are more dependent on the apical stem than is the in vivo rescue assay. Consistent with this explanation, *ls*3 and *ls*5 RNAs, which are severely defective in the rescue assay but less defective in DAI binding (17, 18), were somewhat more effective than *ls*1 RNA at preventing DAI activation in vitro (Fig. 7). Unlike *dl*1, these two linker-scanning mutants possess a wild-type apical stem. Alternatively, the anomalous behavior of *dl*1 might be related to the proximity of the apical stem to the central domain. As in *del*53-80, the residual stem in *dl*1 RNA is adjacent to the central domain (17). This explanation would strengthen the conclusion that function in vitro requires the duplexed part of the apical stem to be separated from the central domain by a spacer region of 5 to 10 nt.

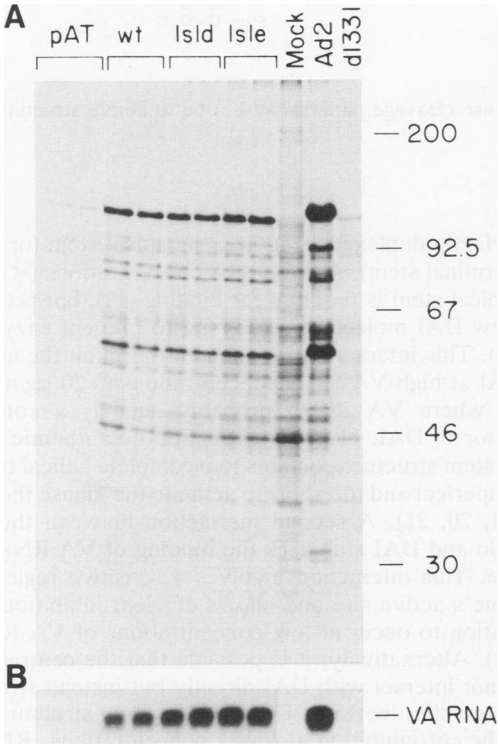


FIG. 5. Rescue of protein synthesis by *ls*1d and *ls*1e. (A) Cells were transfected with 15 μg of the plasmids indicated, and protein synthesis was analyzed as in Fig. 3A. Plasmid pAT153, a derivative of pBR322, served as a negative control. The positions of molecular mass standards (in kilodaltons) are shown. (B) Cytoplasmic RNA from each culture was fractionated and transferred to nitrocellulose as in Fig. 3B. The blot was probed with antisense VA RNA produced from the vector p5′VA (8). An autoradiogram of the VA RNA region is shown.

## DISCUSSION

Previous work revealed that two elements of secondary structure, the apical stem-loop and the central domain, are important for VA $RNA_I$ function. The apical stem-loop is required, at least in vitro, for the efficient binding of VA RNA to its target, the interferon-induced eIF-2 kinase DAI (17), while the central domain is required for inhibition of DAI activation in vivo (5, 18). Little was known about the precise structures and sequences that are involved, although it was evident that certain limited alterations in the apical stem are tolerated, including small changes in the loop, slight shortening of the stem, and some changes in the sequences which comprise the stem-loop (5, 15, 18). Here, we address the sequence and structural features of the apical stem that are important for VA $RNA_I$ function.

The starting points for this study were a substitution mutant, *ls*1, which replaces 6 bases near the base of the apical stem, and a pair of deletion mutants, A2dl2 and *dl*1, which together remove 12 nt from the top and middle of the stem (Fig. 1B). The *ls*1 mutation leads to widespread rearrangements of RNA secondary structure and eliminates function in transient expression assays, whereas the deletions give rise to minor structural changes that are fully compatible with function in vivo (17, 18). We have made eight additional mutants based on these ones to define the determinants that influence VA RNA structure and function.

**Structural implications.** Powerful support for the proposed pairing scheme (5, 18) (Fig. 1A) comes from the observation that the *ls*1c substitution, which introduces compensating base changes on the opposite side of the apical stem from the *ls*1 mutation, fully restores the structure of the molecule. Also consistent with the structural model are the consequences of the *ls*1a and *ls*1b substitutions: the former creates the predicted bifurcation while the latter is too slight to result in any perceptible change in structure. Similarly, the elimination of 28 nt in *del*53-80 results in the expected truncation of the apical stem. In this mutant and in *ls*1a to -c, structural changes elsewhere in the molecule are small or nonexistent.

Three other mutations, *ls*1d and *ls*1e (which each substitute 4 nt in the apical stem) and *del*73-84 (which eliminates all 12 of the bases missing in both A2dl2 and *dl*1), display the modified apical stem structure first seen in A2dl2 RNA. Thus, it seems that VA $RNA_I$ adopts the ostensibly more stable pairing scheme containing six G-C pairs under the influence of a variety of changes in the apical stem. Unlike A2dl2, however, these mutations engender some changes in neighboring structures at the base of the apical stem and in the central domain. The changes are relatively minor, and the overall structure of the molecule remains recognizable. On the other hand, the *del*49-60 deletion removes 12 nt, including the CCGGGG sequence that forms the 5′ side of the six G-C pairs, and consequently the apical stem is severely disrupted. Furthermore, the central domain is extensively disturbed. Taken together, these observations sug-

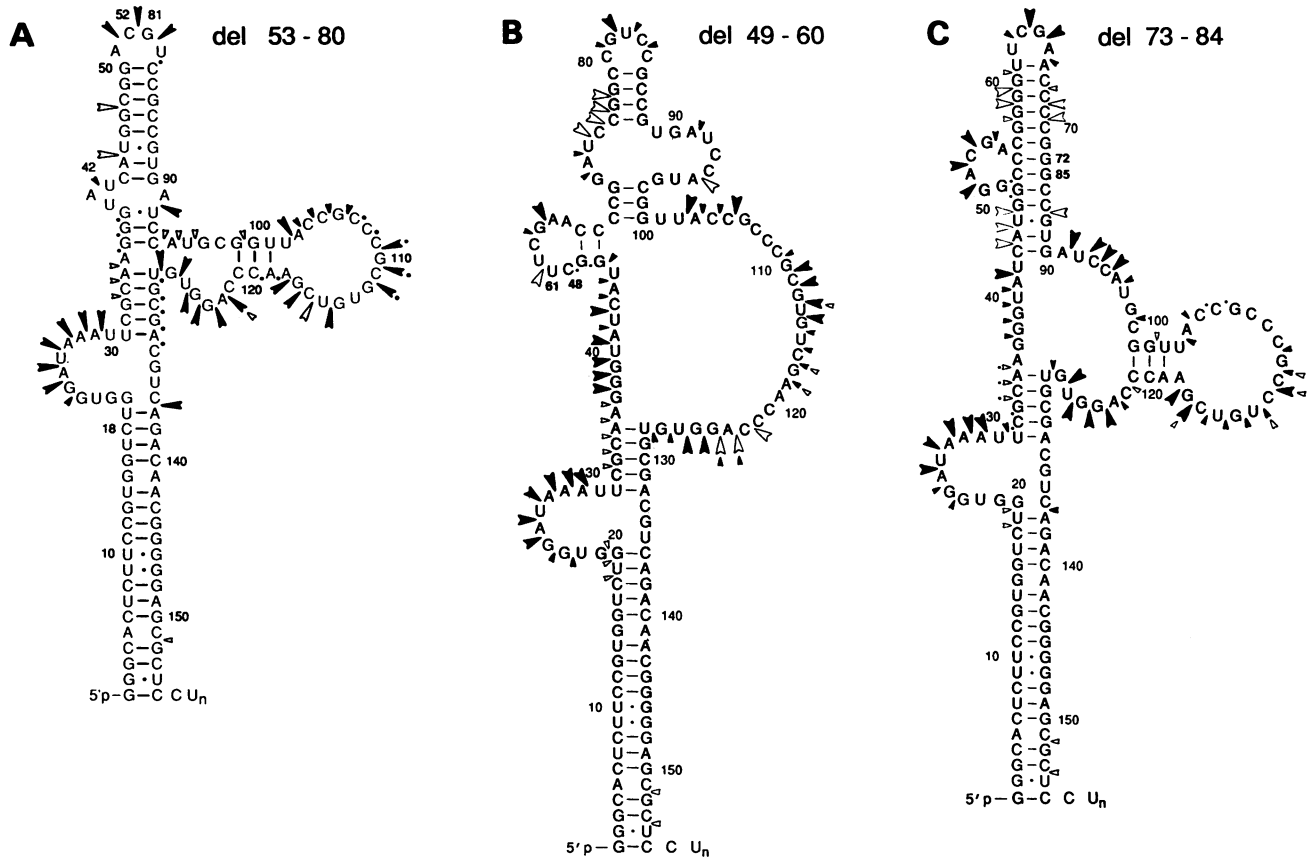


FIG. 6. Secondary structure models for VA RNA deletion mutants. Nuclease cleavage patterns were used to derive structures for the mutants *del*53-80 (A), *del*49-60 (B), and *del*73-84 (C).

gest that the stability of the central domain depends on duplex structure at the base of the apical stem.

**Functional implications.** The two mutants possessing an undisturbed secondary structure, *ls*1b and *ls*1c, rescue protein synthesis in Ad5*dl*331-infected cells as efficiently as wild-type VA $RNA_I$. Together with earlier findings (15, 18), this suggests that there is no specific sequence requirement in the apical stem. The other mutants in this series, *ls*1a, *ls*1d, and *ls*1e, were about half as active as wild-type VA RNA in the rescue assay. One of these mutants (*ls*1d) also exhibited changes in the central domain, but it is unlikely that these are responsible for decreased function, since structural changes of similar magnitude are fully tolerated in a series of mutants that we have generated in the central domain (22). Moreover, the reduced activity of *ls*1a was not accompanied by obvious changes in the central domain, and in *ls*1e the changes were minor. Thus, our data argue that the duplex structure at the base of stem 4 contributes to the integrity of the central domain and also plays a more direct role in VA RNA function. Results of kinase inhibition assays corroborate the notion that both the central domain and apical stem participate in VA RNA function and further suggest that the length of the duplex region and the spacing between the two elements may be critical.

How does VA $RNA_I$ inhibit the activation of DAI? Our data are consistent with a two-step model involving interactions between DAI and both the apical stem and the central domain. First, VA $RNA_I$ binds to the kinase by utilizing its imperfectly duplexed structure, the apical stem (or possibly the terminal stem). At low RNA concentrations (<1 μg/ml), the apical stem is required for binding (17), but presumably too few DAI molecules are bound to prevent enzyme activation. This interaction is sufficient to inhibit the activation of DAI at high VA RNA concentrations (>20 μg/ml), however, where VA $RNA_I$ probably acts as a competitive inhibitor of DAI, blocking activation by authentic dsRNA. Each stem structure contains two complete helical turns that are imperfect and too short to activate the kinase themselves (2, 14, 20, 21). A second interaction between the central domain and DAI stabilizes the binding of VA $RNA_I$ to the kinase. This interaction involves a sensitive region of the enzyme's active site and allows efficient inhibition of DAI activation to occur at low concentrations of VA RNA (≤5 μg/ml). Alternatively, it is possible that the central domain does not interact with DAI directly but instead strengthens the interaction between DAI and the stem structure, allowing efficient inhibition at lower concentrations. RNA most commonly conforms to an A-form helix, which has a deep, narrow, major groove that is not favorable for protein binding. Perhaps the central domain induces a conformational change in the helix, thereby increasing its accessibility to protein contacts as suggested for similar structures in rRNA (3). In either case, our data support the idea that paired regions in the apical stem contribute to both the structure and function of VA $RNA_I$.

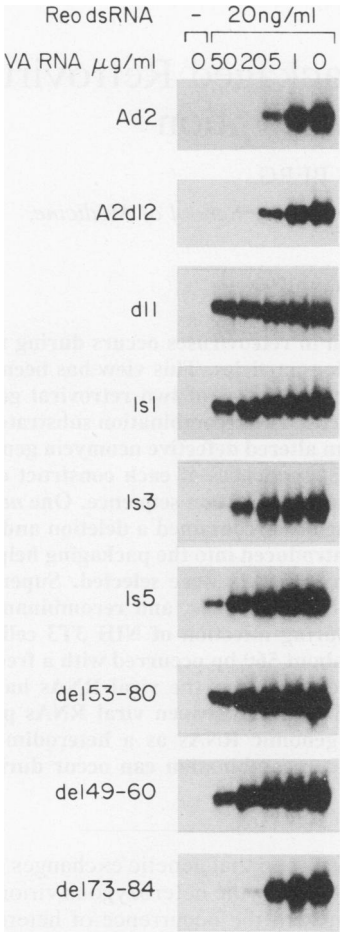


FIG. 7. Inhibition of DAI autophosphorylation by mutant VA RNAs. Wild-type Ad2 VA $RNA_I$ and mutant VA RNAs were tested for their abilities to inhibit the activation of DAI by reovirus dsRNA. Each panel contains a section of the autoradiogram from a representative kinase assay. Gels were exposed for various times to obtain comparable intensities in the 0 lanes. Concentrations of VA RNA (50, 20, 5, 1, and 0 μg/ml) are indicated above lanes.

## ACKNOWLEDGMENTS

We are indebted to L. Manche and R. Packer for technical assistance and to J. Maizel and Y. Ma for discussion and help with RNA folding programs.

This work was supported by grant CA13106 from the National Cancer Institute.

## REFERENCES

1. **Akusjärvi, G., M. B. Mathews, P. Andersson, B. Vennström, and U. Pettersson.** 1980. Structure of genes for virus-associated $RNA_I$ and $RNA_{II}$ of adenovirus type 2. Proc. Natl. Acad. Sci. USA **77**:2424–2428.
2. **Baglioni, C., S. Benvin, P. A. Maroney, M. A. Minks, T. W. Nilsen, and D. K. West.** 1980. Interferon-induced enzymes: activation and role in the antiviral state. Ann. N.Y. Acad. Sci. **350**:497–509.
3. **Draper, D. E.** 1989. How do proteins recognize specific RNA sites? New clues from autogenously regulated ribosomal proteins. Trends Biochem. Sci. **14**:335–338.
4. **Fowlkes, D. M., and T. Shenk.** 1980. Transcriptional control regions of the adenovirus VAI RNA gene. Cell **22**:405–413.
5. **Furtado, M. R., S. Subramanian, R. A. Bhat, D. M. Fowlkes, B. Safer, and B. Thimmappaya.** 1989. Functional dissection of adenovirus VAI RNA. J. Virol. **63**:3423–3434.
6. **Ghadge, G. D., S. Sathyamangalam, M. G. Katze, and B. Thimmappaya.** 1991. Binding of the adenovirus VA RNA to the interferon-induced 68-kDa protein kinase correlates with function. Proc. Natl. Acad. Sci. USA **88**:7140–7144.
7. **Guilfoyle, R., and R. Weinmann.** 1981. Control region for adenovirus VA RNA transcription. Proc. Natl. Acad. Sci. USA **78**:3378–3382.
8. **Herrmann, C. H., and M. B. Mathews.** 1989. The adenovirus E1B 19-kilodalton protein stimulates gene expression by increasing DNA levels. Mol. Cell. Biol. **9**:5412–5423.
9. **Jacobson, A., L. Good, J. Simonetti, and M. Zuker.** 1984. Some simple computational methods to improve the folding of large RNAs. Nucleic Acids Res. **12**:45–66.
10. **Kean, J. M., and D. E. Draper.** 1985. Secondary structure of a 345-base RNA fragment covering the S8/S15 protein binding domain of *Escherichia coli* 16S ribosomal RNA. Biochemistry **24**:5052–5061.
11. **Kostura, M., and M. B. Mathews.** 1989. Purification and activation of the double-stranded RNA-dependent eIF-2 kinase DAI. Mol. Cell. Biol. **9**:1576–1586.
12. **Kunkel, T. A.** 1985. Rapid and efficient site-specific mutagenesis without phenotypic selection. Proc. Natl. Acad. Sci. USA **82**:488–492.
13. **Ma, F., and M. B. Mathews.** Unpublished data.
14. **Manche, L., and M. B. Mathews.** Unpublished data.
15. **Mathews, M. B., and T. Grodzicker.** 1981. Virus-associated RNAs of naturally occurring strains and variants of group C adenoviruses. J. Virol. **38**:849–863.
16. **Mathews, M. B., and T. Shenk.** 1991. Adenovirus virus-associated RNA and translational control. J. Virol. **65**:5657–5662.
17. **Mellits, K. H., M. Kostura, and M. B. Mathews.** 1990. Interaction of adenovirus VA $RNA_I$ with the protein kinase DAI: non-equivalence of binding and function. Cell **61**:843–852.
18. **Mellits, K. H., and M. B. Mathews.** 1988. Effects of mutations in stem and loop regions on the structure and function of adenovirus VA $RNA_I$. EMBO J. **7**:2849–2859.
19. **Mellits, K. H., T. Pe'ery, L. Manche, H. D. Robertson, and M. B. Mathews.** 1990. Removal of double-stranded contaminants from RNA transcripts: synthesis of adenovirus VA $RNA_I$ from a T7 vector. Nucleic Acids Res. **18**:5401–5406.
20. **Minks, M. A., D. K. West, S. Benvin, and C. Baglioni.** 1979. Structural requirements of double-stranded RNA for the activation of 2′,5′-oligo(A) polymerase and protein kinase of interferon-treated HeLa cells. J. Biol. Chem. **254**:10180–10183.
21. **Minks, M. A., D. K. West, S. Benvin, J. J. Greene, P. O. P. Ts'o, and C. Baglioni.** 1980. Activation of 2′,5′-oligo(A) polymerase and protein kinase of interferon treated HeLa cells by 2′-O′ methylated poly(inosinic acid):poly(cytidylic acid). J. Biol. Chem. **255**:6403–6407.
22. **Pe'ery, T., K. H. Mellits, and M. B. Mathews.** Unpublished data.
23. **Rohan, R. M., and G. Ketner.** 1987. A comprehensive collection of point mutations in the internal promoter of the adenoviral $VA_I$ gene. J. Biol. Chem. **262**:8500–8507.
24. **Sanger, F., S. Nicklen, and A. R. Coulson.** 1977. DNA sequencing with chain-terminating inhibitors. Proc. Natl. Acad. Sci. USA **74**:5463–5467.
25. **Thimmappaya, B., C. Weinberger, R. J. Schneider, and T. Shenk.** 1982. Adenovirus VAI RNA is required for efficient translation of viral mRNAs at late times after infection. Cell **31**:543–551.
26. **Wu, G.-J., J. F. Railey, and R. E. Cannon.** 1987. Defining the functional domains in the control region of the adenovirus type 2 specific VARNA1 gene. J. Mol. Biol. **194**:423–442.
27. **Zain, S., T. R. Gingeras, P. Bullock, G. Wong, and R. E. Gelinas.** 1979. Determination and analysis of adenovirus-2 DNA sequences which may include signals for late messenger RNA processing. J. Mol. Biol. **135**:413–433.
28. **Zoller, M. J., and M. Smith.** 1984. Oligonucleotide-directed mutagenesis: a simple method using two oligonucleotide primers and a single-stranded DNA template. DNA **3**:479–488.
29. **Zuker, M., and P. Stiegler.** 1981. Optimal computer folding of large RNA sequences using thermodynamics and auxiliary information. Nucleic Acids Res. **9**:133–148.